

Dicarbonylrhodium(I) complexes of aminophenols and their catalytic carbonylation reaction

Manab Sharma¹, Bhaskar J. Sarmah¹, Pradip Bhattacharyya², Ramesh C. Deka³ and Dipak K. Dutta^{1*}

¹Material Science Division, Regional Research Laboratory (CSIR), Jorhat-785 006, Assam, India

²Department of Chemistry, Gauhati University, Guwahati, Assam, India

³Department of Chemical Sciences, Tezpur University, Tezpur, Assam, India

Received 21 November 2006; Accepted 24 November 2006

The complexes $[\text{Rh}(\text{CO})_2\text{CIL}](1)$, where L = 2-aminophenol (a), 3-aminophenol (b) and 4-aminophenol (c), have been synthesized and characterized. The ligands are coordinated to the metal centre through an N-donor site. The complexes 1 undergo oxidative addition (OA) reactions with various alkyl halides (RX) like CH_3I , $\text{C}_2\text{H}_5\text{I}$ and $\text{C}_6\text{H}_5\text{CH}_2\text{Cl}$ to produce Rh(III) complexes of the type $[\text{Rh}(\text{CO})(\text{COR})\text{XCIL}]$, where R = $-\text{CH}_3$ (2), $-\text{C}_2\text{H}_5$ (3), X = I; R = $\text{C}_6\text{H}_5\text{CH}_2-$ and X = Cl (4). The OA reaction with CH_3I follows a two-stage kinetics and shows the order of reactivity as $1b > 1c > 1a$. The minimum energy structure and Fukui function values of the complexes 1a–1c were calculated theoretically using a DND basis set with the help of Dmol³ program to substantiate the observed local reactivity trend. The catalytic activity of the complexes 1 in carbonylation of methanol, in general, is higher (TON 1189–1456) than the species $[\text{Rh}(\text{CO})_2\text{I}_2]^-$ (TON 1159). Copyright © 2007 John Wiley & Sons, Ltd.

KEYWORDS: rhodium complexes; aminophenol; oxidative addition; carbonylation of alcohols; DFT calculations

INTRODUCTION

Methanol is a readily available, cheap resource of organic compounds and its conversion to value-added products is becoming an attractive area of industrial chemistry. Carbonylation of methanol to ethanoic acid by Monsanto's species, $[\text{Rh}(\text{CO})_2\text{I}_2]^-$, is one of the most successful applications of homogeneous catalysis in industry.¹ Considerable efforts have been devoted to improving the catalyst by incorporating different ligands^{2–10} in the metal complex. In this respect, rhodium(I) complexes containing different types of nitrogen donor ligands have aroused considerable interest because of their structural novelty, stability and reactivity. In the field of synthetic organometallic chemistry, the N-donor ligands have recently gained much attention, although they are 'Hard donors' and stabilize both high and low oxidation

states.^{11–16} In contrast to the phosphorus atom, the nitrogen atom has no low-lying d-orbitals available and therefore nitrogen-containing ligands have only σ -donor characteristics and no π -acceptor properties. The metal–nitrogen bond has more pronounced ionic character than the metal–phosphorus bond. A number of such N-donor ligands have been explored and designed^{17–22} to minimize the hardness of the donor site. There are some preliminary reports of rhodium and iron complexes of aminophenol ligands,^{23,24} but a systematic study of reactivity of these complexes towards various electrophiles, catalytic applications and the theoretical aspects has not been carried out so far. In view of the above, a series of rhodium carbonyl complexes of 2-, 3- and 4-aminophenol ligands have been synthesized to study the effect of $-\text{OH}$ groups at different positions of benzene ring on the electron-donating capacity of the N-donor site and to evaluate the catalytic activities of the complexes towards carbonylation of methanol. Moreover, in recent years the computational methods are becoming a very powerful tools for detailed understanding of structure and reactivity of inorganic complexes.^{25–29} Therefore, in this communication we have also performed density function theory (DFT) calculations on the complexes to correlate our experimental findings.

*Correspondence to: Dipak K. Dutta, Material Science Division, Regional Research Laboratory (CSIR), Jorhat-785 006, Assam, India. E-mail: dipakkrdutta@yahoo.com

Contract/grant sponsor: The Department of Science and Technology, New Delhi.

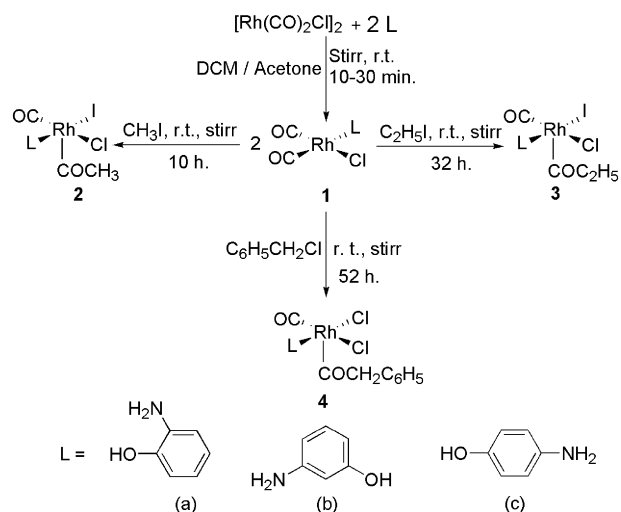
Contract/grant sponsor: DST-International, New Delhi.

Contract/grant sponsor: Oil Industry Development Board, Ministry of Petroleum and Natural Gas, New Delhi.

RESULTS AND DISCUSSION

Synthesis and characterization

The rhodium dimer, $[\text{Rh}(\text{CO})_2\text{Cl}]_2$, reacts with two molar equivalent of the ligands **a–c** to give the complexes of the type $[\text{Rh}(\text{CO})_2\text{ClL}](1)$, where $L = 2\text{-aminophenol (a)}$, 3-aminophenol (b) and 4-aminophenol (c) (Scheme 1). Elemental analyses of the complexes were determined and the results match well with the calculated values. IR spectra of the complexes **1** show two almost equal intense terminal $\nu(\text{CO})$ bands in the range $1999\text{--}2087\text{ cm}^{-1}$, indicating *cis*-disposition of the two CO groups.^{30–32} In the free ligands **a–c**, the $\nu(\text{NH}_2)$ bands occur in the range $3282\text{--}3376\text{ cm}^{-1}$ which on complexation shows a shift of about $74\text{--}171\text{ cm}^{-1}$ towards lower wave number. This indicates that, in the complexes **1**, the ligands are coordinated through N donor sites. It is interesting to note that the $\delta(\text{OH})$ band of the ligands **a** and **b** occurred at 1603 cm^{-1} whereas for **c** it exhibited at 1614 cm^{-1} . The lower frequency of $\delta(\text{OH})$ band for the ligands **a** and **b** may be due to high possibility of formation of intra/intermolecular hydrogen bonding. In case of ligand **c**, as the $-\text{OH}$ and $-\text{NH}_2$ groups are apart from each other, the possibility of forming intra-molecular hydrogen bonding is unlikely. Upon complexation with these ligands (**a–c**), the $\delta(\text{OH})$ values does not show any characteristic shift towards lower frequency, suggesting that the $-\text{OH}$ group remains free; rather the ligands **a** and **b** show a small shift towards high frequency range, which is due to breaking of hydrogen bonding.³³ The effect of hydrogen bonding was further corroborated by the $^1\text{HNMR}$ spectra of these free ligands. The $^1\text{HNMR}$ spectra of the free ligands **a**, **b** and **c** show singlets at δ 5.19, 4.52 and 8.25 ppm for $-\text{NH}_2$ protons, which show a downfield shift of about $0.43\text{--}1.32\text{ ppm}$ when they are involved in complex formation. These clearly indicate that the coordination to the metal centre in the complexes **1** takes place through the N-donor site. On the other hand, the $-\text{OH}$ protons of the ligands resonate at δ 4.18, 3.28 and 3.08 ppm for **a**, **b** and **c** respectively. Among the ligands, the $-\text{OH}$ proton for **a** resonates at the downfield region compared with the other ligands and thus further corroborates the possibility of involvement of intra- and inter-molecular hydrogen bonding between the $-\text{OH}$ proton and $-\text{NH}_2$ group. It is a well known fact that hydrogen bonding involves electron cloud transfer from the hydrogen atom to the neighbouring atom and hence the hydrogen atom experiences a net deshielding effect.³⁴ Thus, at high concentration of hydrogen bonding, $-\text{OH}$ protons resonate at high δ value. The reverse situation is observed in the case of minimization of hydrogen bonding. Accordingly, the extent of hydrogen bonding decreases when the ligands form complex through the N-atom. This was substantiated by the upfield shift of the $-\text{OH}$ proton in complex **1a**. In case of ligand **b**, the extent of intra-molecular hydrogen bonding will be less and therefore the $-\text{OH}$ proton shows less upfield shift. While in complex **1c**, the $-\text{OH}$ proton is involved neither in hydrogen bonding nor in coordination to the metal centre, and thus does not show any appreciable shift.



Scheme 1. Synthesis of rhodium carbonyl complexes containing aminophenol ligands and their oxidative reactivity.

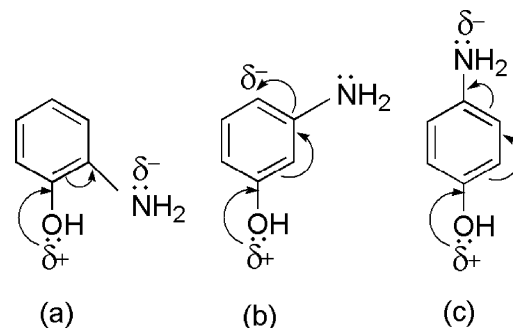
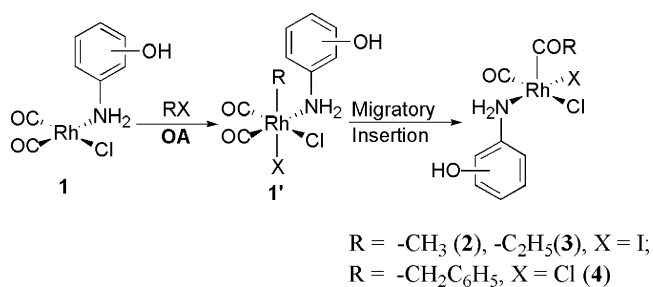


Figure 1. Effect of electron density on the N-atom by electron donating $-\text{OH}$ group in the benzene ring.

Again, the electron donating capacity of the $-\text{NH}_2$ group is influenced through the resonance effect caused by the presence of donor $-\text{OH}$ group at different positions in the benzene ring of the ligands, as shown in Fig. 1. Thus, the ligands **a** and **c** should have stronger electron donating capacity than the ligand **b**. Further, the electron density on the N-atom was calculated by an *ab-initio* Hartree–Fock (HF)³⁵ method and was found to be -0.403974 , -0.382817 and -0.383999 for the ligand **a**, **b** and **c**, respectively. It is therefore clear that the presence of $-\text{OH}$ group at 2- and 4-positions enhances the electron density on the N-atom and follows the order 2-aminophenol (**a**) > 4-aminophenol (**c**) > 3-aminophenol (**b**). It is observed that the order of appearance of $\nu(\text{CO})$ bands in respect of energy is **1a** > **1c** > **1b**, which could not be explained from the electron donating ability, as indicated above. The proper interpretation is likely to be associated with other factors like phenoxide formation, field effect and mutual coupling,^{23,24,34,36} which need be considered for total and perfect analysis of the observed $\nu(\text{CO})$ values.



Scheme 2. OA reaction of **RX** with complexes **1**.

Reactivity of the complexes **1** towards various electrophiles

The complexes **1** undergo OA reactions with various electrophiles like CH_3I , $\text{C}_2\text{H}_5\text{I}$ and $\text{C}_6\text{H}_5\text{CH}_2\text{Cl}$. It is assumed that the OA of alkyl halides to the Rh(I) centre forms a six coordinated Rh(III) alkyl intermediate species before forming the acyl complexes **2–4** (Scheme 2). During the addition, the alkyl and halo groups of the electrophiles may occupy *cis*- or *trans*- coordination sites, leading to formation of several possible isomers of the intermediates. These intermediates then undergo migratory insertion reaction to form five coordinated rhodium(III) acyl complexes of the type $[\text{Rh}(\text{CO})(\text{COR})\text{XCIL}]$, where $R = -\text{CH}_3$ (**2**), $-\text{C}_2\text{H}_5$ (**3**), $X = \text{I}$ and $R = \text{C}_6\text{H}_5\text{CH}_2$ (**4**), $X = \text{Cl}$ (Scheme 2). The IR spectra of the complexes **2** show only a single terminal $\nu(\text{CO})$ band in the range $2065\text{--}2073\text{ cm}^{-1}$. The high value of the terminal $\nu(\text{CO})$ band indicates the formation of the oxidized products. Apart from these, a new $\nu(\text{CO})$ band appeared in the range $1710\text{--}1731\text{ cm}^{-1}$ due to the formation of the acyl carbonyl group. The oxidized products show the $\delta(\text{OH})$ and $\nu(\text{NH}_2)$ bands in almost the same range as that of the complexes **1**. These indicate that in complexes **2** ligands remain in the N-coordinated mode, like those in complexes **1**. The ^1H NMR spectra of the $-\text{NH}_2$ and $-\text{OH}$ protons are found to resonate almost in the same region as that of the complex **1**, only with a slight downfield shift. Apart from these, the complexes **2** show a new singlet resonance in the region δ 2.32–2.97 ppm indicating the formation of $-\text{COCH}_3$ group. In a similar manner, the IR spectra of the complexes **3** and **4** show two different $\nu(\text{CO})$ bands in the range $2045\text{--}2078\text{ cm}^{-1}$ and $1693\text{--}1751\text{ cm}^{-1}$ which are attributable to the terminal and acyl $\nu(\text{CO})$ values, respectively, for the rhodium(III) acyl species. The bonding of the ligands in complexes **3** and **4** are the same as that of the parent complexes **1**, substantiated by the IR spectroscopy. The ^1H NMR spectra of the complexes **3** show a triplet in the range δ 1.54–1.92 ppm and a quartet at around δ 2.34–2.54 ppm for methyl and methylene protons, respectively, of the $-\text{COCH}_2\text{CH}_3$ group with the other characteristic resonance of the ligands. The complex **4** shows a singlet at around δ 3.55 ppm, which corresponds to the methylene protons of the $-\text{COCH}_2\text{C}_6\text{H}_5$ group. The deshielded resonance of the $-\text{COCH}_2-$ protons

is probably due to the presence of electron withdrawing phenyl group. Most of the five-coordinated carbonyl-Rh(III)-acyl complexes reported are square pyramidal in nature;^{37–40} it is likely that the acyl complexes **2–4** would also have a similar geometry. The presence of a single high terminal $\nu(\text{CO})$ value is consistent with CO group *trans* to a weak *trans* influencing chloride.³⁷ On the other hand, the high *trans* influencing nature of the acetyl group favours the epical position *trans* to the vacant site.^{40,41} Therefore, based on the IR and NMR data, the proposed structure of the complexes is shown in the Scheme 2. However, our attempt to isolate suitable crystals for X-ray crystal structure determination was not successful.

Kinetic experiments were carried out to evaluate the effect of various ligands on the OA reactivity of the complexes **1** towards CH_3I . The reaction kinetics were monitored by following the simultaneous decay of the terminal $\nu(\text{CO})$ band (lower value) in the region $1999\text{--}2015\text{ cm}^{-1}$ for the complexes **1a–1c** and the formation of acyl $\nu(\text{CO})$ in the region $1710\text{--}1731\text{ cm}^{-1}$ for the complexes **2a–2c** by recording IR spectra in a definite time intervals. A typical set of IR spectra of the OA reaction for the complexes **1b** is shown in Fig. 2. It is worth mentioning here that the bands of the complexes **1** in CH_3I show a slightly higher energy shift ($\sim 5\text{ cm}^{-1}$). During the progress of the reaction, a new band appeared and thereafter disappeared in the region $2024\text{--}2034\text{ cm}^{-1}$ (Fig. 2). A plot was made for absorbance against time (Fig. 3) for (i) the decay of the terminal $\nu(\text{CO})$ bands ($1999\text{--}2015\text{ cm}^{-1}$) of **1** and (ii) the growth of the new terminal $\nu(\text{CO})$ bands ($2024\text{--}2034\text{ cm}^{-1}$) followed by decay. From the plot, it is observed that, for all the complexes **1a–1c**, the OA reactions proceed with an initial slow step followed by a faster one till the end of reaction. The rate of decrease of intensity of the

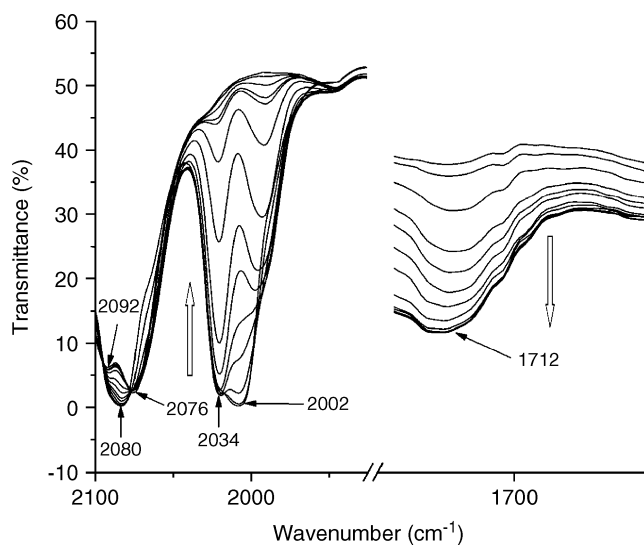


Figure 2. A typical sets of IR spectra ($\nu(\text{CO})$) showing the formation and decay of different species during OA reaction of **1b** with CH_3I .

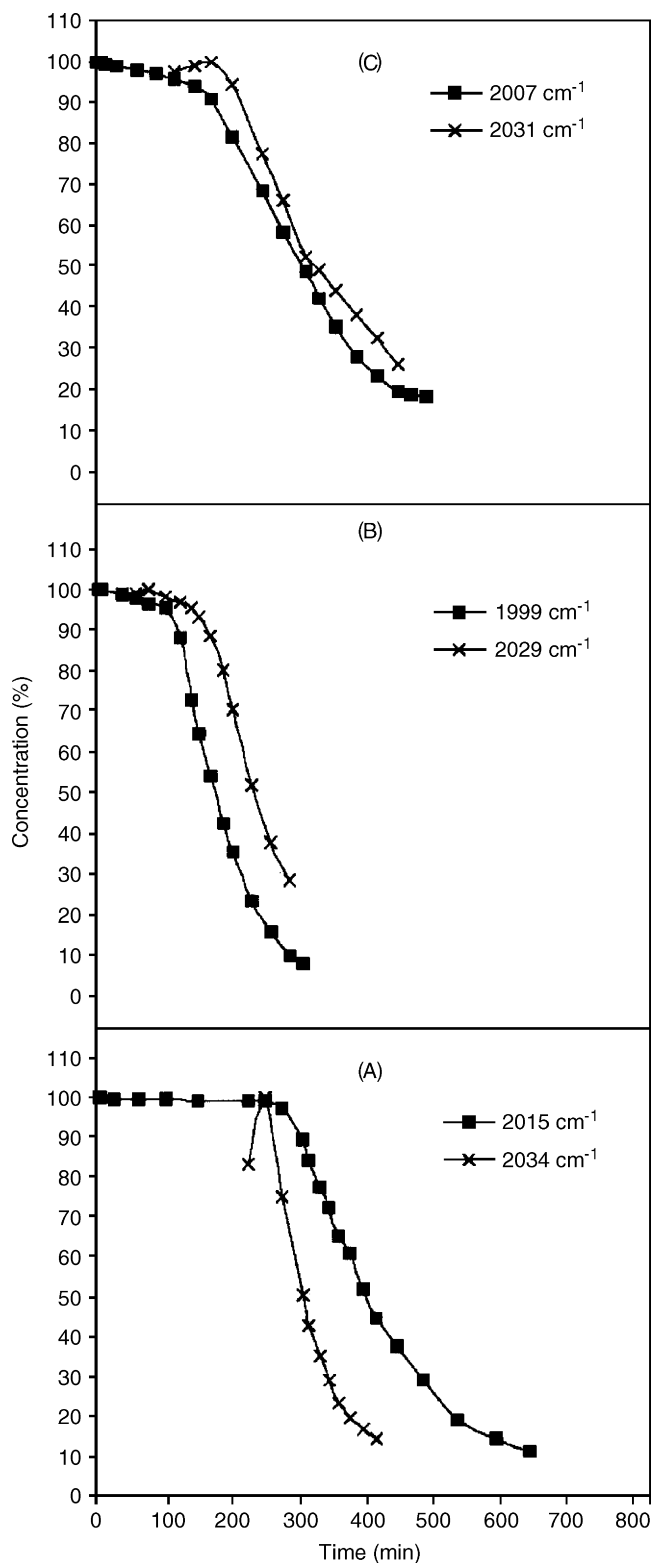


Figure 3. The absorbance of $\nu(\text{CO})$ against time for the different carbonyl species: decay (■) of the terminal $\nu(\text{CO})$ band of complexes **1a** (A), **1b** (B) and **1c** (C); (×) variation of intensity of terminal $\nu(\text{CO})$ band of complexes **1'a** (A), **1'b** (B) and **1'c** (C).

parent complex bands (1 ml CH_3I) of **1a** at 2015 cm^{-1} was very slow up to a period of about 250 min [Fig. 3(A)] and thereafter proceeds rapidly. Similarly, for the complexes **1b** and **1c** up to a period of about 110 [Fig. 3(B)] and 185 min [Fig. 3(C)], respectively, the progress of the reactions was very slow. It is also observed that, within this period, the corresponding formation of the acyl complexes were negligible. On the other hand, the intensity of the new $\nu(\text{CO})$ bands increased and attained a maximum at around 250, 95 and 185 min (Fig. 3) for the intermediate complexes **1'a**, **1'b** and **1'c** respectively (Scheme 2) and, with the progress of the reaction, the intensity of these bands decreased in a similar way to that of the parent complexes **1**. The intensity of the new $\nu(\text{CO})$ bands around $2024\text{--}2034\text{ cm}^{-1}$ could not be measured at the very initial period of the reaction since it was almost enveloped by the lower $\nu(\text{CO})$ band of the complexes **1** and hence the plot was made only after a certain progress of the reaction. The higher frequency of the new $\nu(\text{CO})$ bands (range $2024\text{--}2034\text{ cm}^{-1}$) compared with $\nu(\text{CO})$ bands ($1999\text{--}2015\text{ cm}^{-1}$) of the parent complexes **1** and the observed kinetics reveal that the former $\nu(\text{CO})$ bands belong to the hexacoordinated intermediate **1'** (Scheme 2). With respect to assigning the other higher $\nu(\text{CO})$ values of the intermediates, only for **1b** was a new band observed at 2095 cm^{-1} , while for the other two complexes (**1a** and **1c**) these bands are likely to be enveloped by the corresponding $\nu(\text{CO})$ bands of the parent complexes. The initial slow progress of the reactions indicates the involvement of an induction period, during which the intensity of the $\nu(\text{CO})$ bands of the intermediates attains a maximum, which further suggests that a critical concentration factor of these intermediate might be responsible for the sharp enhancement of the rate of the second stage. From Fig. 3, it was observed that the **OA** reactivity of the complexes **1** towards the electrophile, CH_3I , follows the order **1b** > **1c** > **1a** and, in general, the second stages are faster than the first stages. The intermediate **1'a** shows faster decay rate than the parent complex **1a** [Fig. 3(A)]. This can be explained with the help of steric hindrance caused by the presence of the $-\text{OH}$ group at the 2-position in the ligand, which may sterically restrict the path of CH_3I group during the **OA** step to form the hexacoordinated Rh(III) alkyl intermediate **1'a** (Scheme 2). At the same time, after forming the intermediate, a crowded Rh(III) centre tends to facilitate the migratory insertion step to release the steric strain. Thus, it takes longer to attain the maximum concentration of the **1'a**, but once it is reached, the decay is rapid. In case of **1b'** and **1c'** the rate of decay is similar to that of the parent complexes. In order to substantiate the above findings, a theoretical calculation in respect of Fukui function relating to the local reactivity of the complexes has been done. The Fukui function values (Table 1) of the complexes for electrophilic attack on the Rh centre were

Table 1. Some important parameter of the complexes **1a–1c**

Parameters	1a	1b	1c
Optimized energy ^a	-5740.895 792	-5740.886 973	-5740.888 700
Fukui	0.153	0.151	0.149
Function: f^+			
f^{2-}	0.225	0.212	0.210
f^+ / f^{2-}	0.680	0.712	0.709

^a Hartre, f^+ = Fukui function for nucleophilic attack; f^- = Fukui function for electrophilic attack.

found to follow the order **1a** > **1b** > **1c**. Thus, electronically **1a** is more prone to electrophilic attack and was expected to show high reactivity towards the **OA** reaction, but in practice the observed lower reactivity is attributable to the predominating steric factor over electronic one, as explained above. On the other hand, for **1b** and **1c** the electronic factors play a key role as the substituents on the ligands are away from their coordination site and subsequently away from the active Rh centre. Thus, the high philicity of the Rh centre in complex **1b** makes it more prone towards **OA** of CH₃I, which in contrast might tend to reduce the migratory insertion reaction⁴¹ and might lead to initial equilibrium between **1'b** and **1b**. After a certain reaction time when a major portion of **1b** was reacted, the equilibrium was disturbed and the rate of decay of **1'b** became faster. In the case of **1c**, the concentration of the intermediate attained a maximum at about 185 min and thereafter the decay of the intermediate **1c'** and **1c** followed a similar kinetics [Fig. 3(C)].

Carbonylation of methanol

Catalytic carbonylation of methanol to ethanoic acid and its ester was carried out in the presence of complexes **1** and the results are given in Table 2. During 60 min of reaction time (Table 2), 54.54, 65.08 and 53.70% conversions of methanol were obtained with corresponding turn over number (TON) 812, 1004 and 828 for the complexes **1a**, **1b** and **1c**, respectively, which further increases with the increase in reaction time. In general, for a particular reaction time and conditions, complexes **1** show higher catalytic activity over the well-known catalyst precursor [Rh(CO)₂I₂]⁻ generated *in situ* from [Rh(CO)₂Cl]₂.⁴² It has been observed that the efficiency of the catalyst precursors **1** are different and found to follow the order **1b** > **1c** > **1a**. The observed trend in reactivity cannot be explained only from the simple electron donating capacity of the ligand. To explain this, one must consider the steric factors, hydrogen bonding, field effects and phenoxide formation. A cumulative effect of all these might have increased the efficiency of the catalyst **1b** over **1a** and **1c**. From the results it is also observed that, as the reaction time increased, the selectivity of the catalyst towards acid formation increased (Table 2). After completion of the carbonylation reaction of methanol (120 min run), the catalytic solution was evaporated

to dryness to obtain a solid mass that showed multiple $\nu(\text{CO})$ bands that matched well with the spectra of a mixture of parent rhodium(I) carbonyl complexes and rhodium(III) acyl complexes. On recycling the solid mass as catalysts for the second time, nearly the same amount of conversion was found (Table 2), indicating longer durability as well as stability of the catalysts.

Theoretical calculation

To understand the reactivity differences of these complexes, a theoretical calculation was carried out to find out the minimum energy structure (Fig. 4) of the complexes **1a–1c**. The final structure was obtained using a DND basis set with a Dmol³ programme. The complexes were fully optimized and a few selected geometric parameters, i.e. bond length and bond angles are given in Table 3. From the optimized structures of the complexes **1a–1c**, it was observed that the Rh centre lies in a distorted square planer environment with two *cis*-C-atoms of two CO groups, one Cl-atom *trans* to one CO and an N-atom of the ligand *cis*- to the Cl-atom. The Rh(1)–N(1)–C(4) bond angle was found to be 120.13, 118.76 and 116.21° for the complexes **1a**, **1b** and **1c**, respectively. The observed highest bond angle and bond length between the Rh(1) and N(1) for **1a** were attributable to the high steric hindrance due to the presence of the –OH group near to the donor –NH₂ group of the ligand. The Fukui function (FF)⁴³ was also calculated to determine the local reactivity in the complexes. It is known that atom with the higher FF value is highly reactive compared with the other atoms in a molecule.^{43,44} The FF for the Rh atom is given in the Table 1. The results reveal that the ratio of FF values for

Table 2. Results of carbonylation of methanol^a in presence of complexes **1** as catalyst precursors

Catalyst	Duration (min)	Methyl acetate (%)	Acetic acid (%)	Total conversion (%)	TON ^b
1a	60	42.09	12.45	54.54	812
	90	39.65	25.17	64.47	960
	120	36.56	43.29	79.85	1189
	120 ^b	36.59	42.39	78.98	1176
1b	60	50.67	14.41	65.08	1004
	90	31.68	60.22	91.90	1418
	120	28.68	65.72	94.40	1456
	120 ^c	26.65	63.89	90.54	1397
1c	60	45.50	8.20	53.70	828
	90	39.11	23.36	62.47	964
	120	30.95	50.81	81.76	1261
	120 ^c	30.01	49.88	79.89	1232

^a Reaction conditions: catalyst:substrate = 1:1600; temperature, 130 ± 5 °C; pressure, 35 ± 2 bar.

^b TON = mole of product per mole of catalyst; ^c recycled catalyst; TON obtained for precursor [Rh(CO)₂Cl]₂ are 648, 951 and 1159 with corresponding reaction times 60, 90 and 120 min.

nucleophilic attack to electrophilic attack (f^+ / f^{2-}) follows the order $1b > 1c > 1a$. Therefore, for electrophilic attack, the Rh centre of the complex **1b** is more active than the other two complexes and, hence, **1b** is expected to be more reactive towards OA of CH_3I as it involves the initial electrophilic attack by the $-\text{CH}_3$ group followed by transfer of iodine (nucleophilic) to the metal centre.^{45,46} On the other hand, the FF values for electrophilic attack on Rh centre follow the order $1a > 1b > 1c$, but in practice **1b** shows higher reactivity than other two complexes (Tables 1 and 2). To explain these, one needs to consider the steric factors of the complexes as well. From Fig. 4 it is clear that, in **1a**, the Rh centre is at a sterically more hindered situation than in **1b** or **1c** and thus the steric factor might predominate over electronic factors. Therefore, the actual reactivity trend of the complexes **1** depends on both the electronic as well as steric factors.

EXPERIMENTAL

All the solvents used were distilled under N_2 prior to use. Elemental analyses were done on a Perkin-Elmer 2400 elemental analyser. FT-IR spectra ($4000\text{--}400\text{ cm}^{-1}$) were recorded using a Perkin Elmer 2000 spectrophotometer in CHCl_3 and as KBr discs. The ^1H NMR (270 MHz) spectra were recorded in CDCl_3 or in $\text{CH}_3\text{COCH}_3\text{-d}_6$ solution on a Jeol Delta 270 MHz and chemical shifts were reported relative to SiMe_4 as an internal reference. The carbonylation of alcohols were carried out in a 100 cm^3 Teflon-coated high-pressure reactor (HR-100, Berghof, Germany) fitted with a pressure gauge, and the reaction products were analysed by GC (Chemito 8510, FID). $\text{RhCl}_3 \cdot 3\text{H}_2\text{O}$ was purchased from M/s Arrora Matthey Ltd, Kolkata, India. All the ligands were purchased from Aldrich, USA and used as received.

Table 3. Some important bond lengths and bond angles obtained for the complexes **1a–1c** by geometry optimization

Parameters	1a	1b	1c
<i>Bond lengths (Å)</i>			
Rh(1)–N(1)	2.23	2.17	2.19
Rh(1)–C(1)	1.89	1.90	1.89
Rh(1)–C(2)	1.89	1.89	1.89
C(1)–O(1)	1.16	1.16	1.16
C(2)–O(2)	1.15	1.15	1.15
<i>Bond angle (deg)</i>			
N(1)–Rh(1)–C(1)	90.89	90.85	93.58
N(1)–Rh(1)–C(2)	176.17	176.48	173.28
C(1)–Rh(1)–C(2)	92.53	92.67	92.42
N(1)–Rh(1)–Cl(1)	89.34	89.90	82.92
C(1)–Rh(1)–Cl(1)	178.79	177.05	175.68
C(2)–Rh(1)–Cl(1)	87.88	86.60	92.42
Rh(1)–N(1)–C(4)	120.13	118.76	116.21

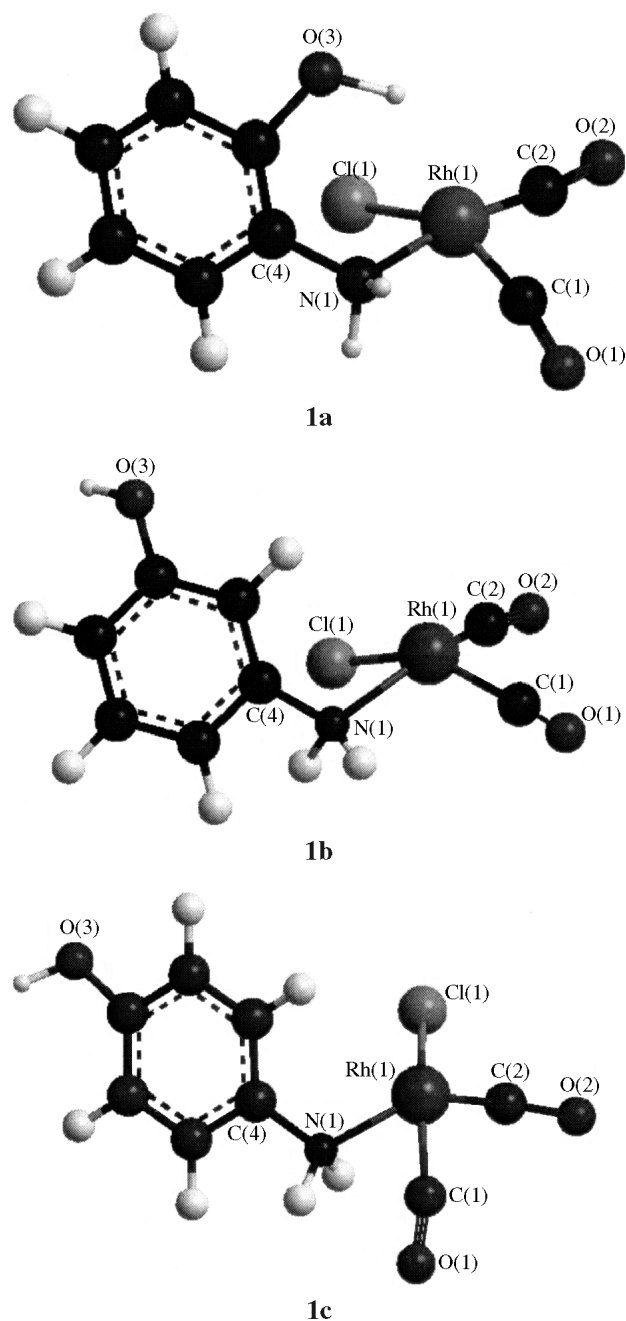


Figure 4. Geometry optimized structures of the complexes **1a–1c**.

Starting material

All the complexes were synthesized from $[\text{Rh}(\text{CO})_2\text{Cl}]_2$, which was prepared by passing CO gas over $\text{RhCl}_3 \cdot 3\text{H}_2\text{O}$ at 100°C .⁴⁷

*Preparation of $[\text{Rh}(\text{CO})_2\text{ClL}]$ (**1**), where $L = 2\text{-aminophenol}$ (**a**), 3-aminophenol (**b**) and 4-aminophenol (**c**)*

$[\text{Rh}(\text{CO})_2\text{Cl}]_2$ was dissolved (10.00 mg, 0.0257 mmol) in CH_2Cl_2 (10 cm^3) and to this an ethanolic solution

(10 cm³) of the corresponding ligands, 2-aminophenol (**a**), 3-aminophenol (**b**) and 4-aminophenol (**c**), (5.55 g, 0.0514 mmol) was added. The reaction mixture was stirred at room temperature (r.t.) for about 30 min and the solvent was evaporated under vacuum. The light reddish colour compound obtained was washed with diethyl ether and kept over silica gel. **1a**: yield 97%. C₈H₇ClINO₃Rh (303.45): calcd C 31.66, H 2.31, N 4.62; found C 31.43, H 2.41, N 4.70%. ¹HNMR (270 MHz, CH₃COCH₃-d₆): δ = 5.62 (s, 2H, NH₂), 3.30 (s, 1H, -OH), 6.28–7.02 (m, 4H, -C₆H₄) ppm. FT-IR (KBr): ν = 2015, 2087 [ν(CO)], 3292, 3232 [ν(NH₂)], 1609 [δ(OH)] cm⁻¹. **1b**: yield 98%. C₈H₇ClINO₃Rh (303.45): calcd C 31.66, H 2.31, N 4.62; found C 31.51, H 2.42, N 4.67%. ¹HNMR (270 MHz, CH₃COCH₃-d₆): δ = 5.84 (bs, 2H, NH₂), 3.25 (s, 1H, -OH), 7.91 (s, H₂, -C₆H₄) 6.82–6.86 (m, H₆/H₄, -C₆H₄), 6.32–6.42 (m, H₅, -C₆H₄) ppm. FT-IR (KBr): ν = 1999, 2074 [ν(CO)], 3252, 3125 [ν(NH₂)], 1605 [δ(OH)] cm⁻¹. **1c**: yield 95%. C₈H₇ClINO₃Rh (303.45): calcd C 31.66, H 2.31, N 4.62; found C 31.53, H 2.29, N 4.58%. ¹HNMR (270 MHz, CH₃COCH₃-d₆): δ = 8.72 (s, 2H, NH₂), 3.10 (s, 1H, -OH), 6.22–7.29 (m, 4H, -C₆H₄) ppm. FT-IR (KBr): ν = 2007, 2080 [ν(CO)], 3259, 3205 [ν(NH₂)], 1611 [δ(OH)] cm⁻¹.

Preparation of [Rh(CO)(COCH₃)ICIL] (2) where L = 2-aminophenol (a), 3-aminophenol (b) and 4-aminophenol (c)

To an acetone solution of the complexes **1** (100.00 mg, 0.3295 mmol in 10 cm³) CH₃I (96.3 mmol, 6 cm³) was added. The reaction mixture was then stirred at r.t. for about 10 h and the solvent was evaporated under vacuum. Yellow-reddish coloured compounds obtained were washed with diethyl ether and kept over silica gel in a desiccator. **2a**: yield 90%. C₉H₁₀ClINO₃Rh (445.36): calcd C 24.27, H 2.25, N 3.15; found C 24.30, H 2.18, N 3.19%. ¹HNMR (270 MHz, CDCl₃): δ = 5.72 (bs, 2H, NH₂), 3.32 (s, 1H, -OH), 6.38–7.12 (m, 4H, -C₆H₄), 2.47 (s, 3H, -COCH₃) ppm. FT-IR (CHCl₃): ν = 2065, 1731 [ν(CO)], 3290, 3212 [ν(NH₂)], 1600 [δ(OH)] cm⁻¹. **2b**: Yield 93%. C₉H₁₀ClINO₃Rh (445.36): calcd. C 24.27, H 2.25, N 3.15; found C 24.23, H 2.28, N 3.10%. ¹HNMR (270 MHz, CDCl₃): δ = 5.91 (bs, 2H, NH₂), 3.31 (s, 1H, -OH), 7.93 (s, H₂, -C₆H₄) 6.78–6.88 (m, H₆/H₄, -C₆H₄), 6.38–6.44 (m, H₅, -C₆H₄), 2.32 (s, 3H, -COCH₃) ppm. FT-IR (CHCl₃): ν = 2073, 1712 [ν(CO)], 3255, 3105 [ν(NH₂)], 1606 [δ(OH)] cm⁻¹. **2c**: yield 88%. C₉H₁₀ClINO₃Rh (445.36): calcd C 24.27, H 2.25, N 3.15; found C 24.31, H 2.15, N 3.11%. ¹HNMR (270 MHz, CDCl₃): δ = 8.77 (bs, 2H, NH₂), 3.12 (s, 1H, -OH), 6.19–7.09 (m, 4H, -C₆H₄), 2.97 (s, 3H, -COCH₃) ppm. FT-IR (CHCl₃): ν = 2067, 1710 [ν(CO)], 3266, 3222 [ν(NH₂)], 1610 [δ(OH)] cm⁻¹.

Preparation of [Rh(CO)(COC₂H₅)ICIL] (3) where L = 2-aminophenol (a), 3-aminophenol (b) and 4-aminophenol (c)

The complexes **1** (100.00 mg, 0.3295 mmol) was dissolved in acetone (10 cm³) and to this C₂H₅I (0.0622 mol, 5 cm³) was added. The reaction mixture was then stirred at r.t. for about 32 h and the solvent was evaporated under

vacuum. Yellow-reddish coloured compounds obtained were washed with diethyl ether and was collected. **3a**: yield 85%. C₁₀H₁₂ClINO₃Rh (459.37): calcd C 26.14, H 2.61, N 3.04; found C 26.02, H 2.53, N 3.05. ¹HNMR (270 MHz, CDCl₃): δ = 5.71 (bs, 2H, NH₂), 3.29 (s, 1H, -OH), 6.22–6.98 (m, 4H, -C₆H₄), 2.54 (q, 2H, -COCH₂CH₃), 1.92 (t, 3H, -COCH₂CH₃) ppm. FT-IR (CHCl₃): ν = 2070, 1751 [ν(CO)], 3291, 3232 [ν(NH₂)], 1598 [δ(OH)]. **3b**: yield 82%. C₁₀H₁₂ClINO₃Rh (459.37): calcd C 26.14, H 2.61, N 3.04; found C 26.05, H 2.58, N 3.00. Calcd for C₁₀H₁₂ClINO₃Rh (%): C, 26.14; H, 2.61; N, 3.04. ¹HNMR (270 MHz, CDCl₃): δ = 5.86 (bs, 2H, NH₂), 3.20 (s, 1H, -OH), 7.94 (s, H₂, -C₆H₄) 6.882–6.96 (m, H₆/H₄, -C₆H₄), 6.38–6.47 (m, H₅, -C₆H₄), 2.34 (q, 2H, -COCH₂CH₃), 1.61 (t, 3H, -COCH₂CH₃) ppm. IR (CHCl₃): ν = 2045, 1693 [ν(CO)], 1604 [δ(OH)], 3224, 3109 [ν(NH₂)]. **3c**: yield 83%. C₁₀H₁₂ClINO₃Rh (459.37): calcd C 26.14, H 2.61, N 3.04; found C 26.22, H 2.48, N 2.98. ¹HNMR (270 MHz, CDCl₃): δ = 8.80 (bs, 2H, NH₂), 3.14 (bs, 1H, -OH), 6.22–6.89 (m, 4H, C₆H₄), 2.36 (q, 2H, -COCH₂CH₃), 1.54 (t, 3H, -COCH₂CH₃) ppm. IR (CHCl₃): ν = 2065, 1732 [ν(CO)], 1611 [δ(OH)], 3264, 3232 [ν(NH₂)].

Preparation of [Rh(CO)(COCH₂C₆H₅)Cl₂L] (4), where L = 2-aminophenol (a), 3-aminophenol (b) and 4-aminophenol (c)

The complexes **1a–1c** (0.3017 mmol) were dissolved in acetone (10 cm³) and to this C₆H₅CH₂Cl (5 cm³) was added. The reaction mixture was then stirred at r.t. for about 52 h and the solvent was evaporated under vacuum. Light brown coloured compounds obtained were washed with diethyl ether and was collected. **4a**: yield 91%. C₁₅H₁₄Cl₂NO₃Rh: calcd C 41.90, H 3.26, N 3.26, found C 41.88, H 3.11, N 3.08. ¹HNMR (270 MHz, CDCl₃): δ = 5.81 (bs, 2H, NH₂), 3.38 (s, 1H, -OH), 6.10–7.15 (m, 4H, C₆H₄), 3.57 (s, 2H, -CH₂-) ppm. IR (CHCl₃): ν = 2077, 1715 [ν(CO)], 1601 [δ(OH)], 3289, 3212 [ν(NH₂)]. **4b**: yield 94%. C₁₅H₁₄Cl₂NO₃Rh: calcd C 41.90, H 3.26, N 3.26, found C 41.79, H 3.21, N 3.18. ¹HNMR (270 MHz, CDCl₃): δ = 5.92 (bs, 2H, NH₂), 3.28 (s, 1H, -OH), 6.24–7.32 (m, 4H, C₆H₄), 3.55 (s, 2H, -CH₂-) ppm. IR (CHCl₃): ν = 2078, 1715 [ν(CO)], 1605 [δ(OH)], 3254, 3209 [ν(NH₂)]. **4c**: yield 92%. C₁₅H₁₄Cl₂NO₃Rh: calcd C 41.90, H 3.26, N 3.26, found C 41.82, H 3.20, N 3.21. ¹HNMR (270 MHz, CDCl₃): δ = 8.81 (bs, 2H, NH₂), 3.23 (s, 1H, -OH), 6.10–7.18 (m, 4H, C₆H₄), 3.57 (s, 2H, -CH₂-) ppm. IR (CHCl₃): ν = 2072, 1720 [ν(CO)], 1610 [δ(OH)], 3268, 3241 [ν(NH₂)].

Spectroscopic data for the ligand 2-aminophenol (a)

¹HNMR (270 MHz, CDCl₃): δ = 5.19 (s, 2H, NH₂), 4.18 (s, 1H, -OH), 6.38–6.95 (m, 4H, C₆H₄) ppm. IR (KBr disc): ν = 1603 [δ(OH)], 3376, 3306 [ν(NH₂)].

Spectroscopic data for the ligand 3-aminophenol (b)

¹HNMR (270 MHz, CDCl₃): δ = 4.52 (s, 2H, NH₂), 3.28 (bs, 1H, -OH), 7.89 (s, H₂, -C₆H₄) 6.72–6.80 (m, H₆/H₄, -C₆H₄), 6.18–6.20 (m, H₅, -C₆H₄) ppm. IR (KBr disc): ν = 1603 [δ(OH)], 3361, 3296 [ν(NH₂)].

Spectroscopic data for the ligand 4-aminophenol (c)

$^1\text{H NMR}$ (270 MHz, CDCl_3): δ = 8.25 (s, 2H, NH_2), 3.08 (bs, 1H, $-\text{OH}$), 6.45–6.88 (m, 4H, C_6H_4) ppm. IR (KBr disc): ν = 1614 [$\delta(\text{OH})$], 3341, 3282 [$\nu(\text{NH}_2)$].

Kinetic experiment

The kinetic experiments of **OA** reaction of complexes **1a–1c** with CH_3I were monitored by using IR spectroscopy in a solution cell (1.0 mm path length). Complexes **1** (10 mg) were taken in a volumetric flask (1 ml) and to it (i) CH_3I (1 ml, 16.05×10^{-3} mol) or (ii) 0.7 ml CH_3I (11.23×10^{-3} mol) and 0.3 ml dichloromethane or (iii) 0.4 ml CH_3I (6.42×10^{-3} mol) and 0.6 ml dichloromethane were added at 25°C . An aliquot of the reaction mixture was transferred by a syringe into the IR cell. The kinetics measurements were made by *in-situ* IR monitoring of the decay of lower energy $\nu(\text{CO})$ band of complexes **1** in the range 1999–2015 cm^{-1} and increasing intensity of the acyl $\nu(\text{CO})$ band in the range 1705–1720 cm^{-1} of $[\text{Rh}(\text{CO})(\text{COCH}_3)\text{Cl}]\text{L}$. A series of spectra were taken at a regular time intervals.

Carbonylation of methanol using complexes 1 as the catalyst precursors

CH_3OH (0.099 mol), CH_3I (0.016 mol), H_2O (0.055 mol) and complexes **1** (0.054 mmol) were taken into the reactor and then pressurized with CO gas (20 bar at r.t., 0.080 mol). The reaction vessel was then placed into the preheated jacket of the autoclave and the reactions were carried out at $130 \pm 5^\circ\text{C}$ (corresponding pressure 35 ± 2 bar) with variation of reaction time. The products were collected and analysed by GC. The recycle experiments were done by maintaining the same experimental conditions as described above with the dark brown solid mass as catalyst obtained by evaporating the carbonylation reaction mixture under reduced pressure.

Computational details

The DFT calculations were performed to determine the optimize structure and reactivity of the complexes **1**. The calculations were carried⁴⁸ out with the programme Dmol³ with DND basis set and HCTH functions. Local reactivity of the molecules was determined with the help of the Fukui Function.⁴³ The different Fukui functions are defined as:

$$f^+(\mathbf{r}) = \rho_{N+1}(\mathbf{r}) - \rho_N(\mathbf{r})$$

for nucleophilic attack

(4)

$$f^-(\mathbf{r}) = \rho_N(\mathbf{r}) - \rho_{N-1}(\mathbf{r})$$

for electrophilic attack

(5)

$$f^0(\mathbf{r}) = (\rho_{N+1}(\mathbf{r}) - \rho_{N-1}(\mathbf{r}))/2$$

for radical attack

(6)

where ρ_N is the electron density at a point r in space around the molecule. $N + 1$ and $N - 1$ correspond to an anion,

with an electron added to the LUMO and a cation with an electron removed from the HOMO of the neutral molecule, respectively.

Acknowledgements

The authors are grateful to Dr P. G. Rao, Director, Regional Research Laboratory (CSIR), Jorhat, India, for his kind permission to publish the work. The authors thank Dr P.C. Borthakur, Head Material Science Division, RRL Jorhat, for his encouragement and support. The Department of Science and Technology (DST), New Delhi, DST-International, New Delhi and the Oil Industry Development Board (OIDB), Ministry of Petroleum and Natural Gas, New Delhi, are acknowledged for their partial financial grant. Special thanks are also due to St Andrews for their help in recording NMR spectra. The author M. Sharma thanks CSIR, New Delhi, for the award of Senior Research Fellowships.

REFERENCES

- Maitlis PM, Haynes A, Sunley GJ, Howard MJ. *J. Chem. Soc., Dalton Trans.* 1996; 2187.
- Wegman RW, Abatjoglou AG, Harrison AM. *J. Chem. Soc., Chem. Commun.* 1987; 1891.
- Dutta DK, Woollins JD, Slawin AMZ, Konwar D, Das P, Sharma M, Bhattacharya P, Aucott SM. *Dalton Trans.* 2003; 2674.
- Sharma M, Kumari N, Das P, Chutia P, Dutta DK. *J. Mol. Catal. A: Chem.* 2002; **188**: 25.
- Das P, Chutia P, Dutta DK. *Chem. Lett.* 2002; 766.
- Das P, Konwar D, Sengupta P, Dutta DK. *Trans. Met. Chem.* 2000; **25**: 426.
- Das P, Boruah M, Kumari N, Sharma M, Konwar D, Dutta DK. *J. Mol. Catal. A: Chem.* 2002; **178**: 283.
- Das P, Sharma M, Kumari N, Konwar D, Dutta DK. *Appl. Organomet. Chem.* 2002; **16**: 302.
- Kumari N, Sharma M, Das P, Dutta DK. *Appl. Organomet. Chem.* 2002; **16**: 258.
- Kumari N, Sharma M, Chutia P, Dutta DK. *J. Mol. Catal. A: Chem.* 2004; **222**: 53.
- Canty AJ. *Acc. Chem. Res.* 1992; **25**: 83.
- Brown BD, Byers PK, Canty AJ. *Organometallics* 1990; **9**: 1231.
- Dehand J, Pfeffer M. *Coord. Chem. Rev.* 1976; **18**: 327.
- Bruce MI. *Angew. Chem.* 1977; **89**: 75.
- Bruce MI. *Angew. Chem. Int. Edn Engl.* 1977; **16**: 73.
- Evans DA, Woerpel KA, Hinman MM, Faul MM. *J. Am. Chem. Soc.* 1991; **113**: 726.
- Britovsek GJP, Gibson VC, Kimberley BS, Maddox PJ, Mc Tavish SJ, Solan GA, White AJP, Williams DJ. *Chem. Commun.* 1998; 849.
- Small BL, Brookhart M, Bennett AMA. *J. Am. Chem. Soc.* 1998; **120**: 4049.
- Borowski AF. *Trans. Met. Chem.* 1984; **9**: 109.
- Nagy-Magos Z, Kvintovics P, Marko L. *Trans. Met. Chem.* 1980; **5**: 186.
- Borowski AF. *Trans. Met. Chem.* 1983; **8**: 266.
- Kwaskowska-Chec E, Trzeciak AM. *Trans. Met. Chem.* 1991; **16**: 212.
- Vasconcellos LCG, Oliveira CP, Castellano EE, Ellena J, Moreira IS. *Polyhedron* 2001; **20**: 493.
- Krylov VK, Kukushkim YuN, Popova NR, Yakovlev VN. *Zh. Obsch. Khim.* 1991; **61**: 1647.
- Privalov T, Linde C, Zetterberg K, Moberg C. *Organometallics* 2005; **24**: 885.

26. Griffin TR, Cook DB, Haynes A, Pearson JM, Monti D, Morris GE. *J. Am. Chem. Soc.* 1996; **118**: 3029.
27. Cavallo L, Sola M. *J. Am. Chem. Soc.* 2001; **123**: 12294.
28. Kinnunen T, Laasonen K. *J. Mol. Struct. (Theochem)* 2001; **540**: 91.
29. Kinnunen T, Laasonen K. *J. Organomet. Chem.* 2003; **665**: 150.
30. Vallarino LM. *Inorg. Chem.* 1965; **4**: 161.
31. Dutta DK, Singh MM. *Trans. Met. Chem.* 1994; **19**: 290.
32. Dutta DK, Singh MM. *Trans. Met. Chem.* 1979; **4**: 230.
33. Dolphine D, Wick A. *Tabulation of IR Spectral Data*. Wiley: New York, 1977; 304.
34. Kemp W. *Organic Spectroscopy*, 3rd edn. ELBS with Macmillan: London, 1991; 132.
35. Levine IN. *Quantum Chemistry*, 4th edn. Prentice-Hall: New Delhi, 1995; 580.
36. Sykes P. *A Guidebook to Mechanism in Organic Chemistry*. Orient Longman: New Delhi, 2001.
37. Adams H, Bailey NA, Mann BE, Manuel CP, Spencer CM, Kent AG. *J. Chem. Soc., Dalton Trans.* 1988; 489.
38. Lindner E, Wang Q, Mayer HA, Fawzi R, Steimann M. *Organometallics* 1993; **12**: 1865.
39. Kent AG, Mann BE, Manuel CP. *J. Chem. Soc., Chem. Commun.* 1985; 728.
40. Gonsalvi L, Adams H, Sunley GJ, Ditzel E, Haynes A. *J. Am. Chem. Soc.* 2002; **24**: 13597.
41. Gonsalvi L, Adams H, Sunley GJ, Ditzel E, Haynes A. *J. Am. Chem. Soc.* 1999; **121**: 11233.
42. Forster D. *J. Am. Chem. Soc.* 1976; **98**: 846.
43. Parr RG, Yang W. *J. Am. Chem. Soc.* 1984; **106**: 4049.
44. Thanikaivelan P, Padmanabhan J, Subramaniam V, Ramasami T. *Theor. Chem. Acc.* 2002; **107**: 326.
45. Douek IC, Wilkinson G. *J. Chem. Soc. A* 1969; 2604.
46. Chauby V, Daran J-C, Berre CS-L, Francois M, Kalck P, Gonzalez OD, Haslam CE, Haynes A. *Inorg. Chem.* 2002; **42**: 3280.
47. McCleverty JA, Wilkinson G. *Inorg. Synth.* 1966; **8**: 221.
48. Delley B. *J. Chem. Phys.* 1990; **92**: 508.